

Accelerated hyaluronan concentration as the primary driver of morbidity and mortality in high-risk COVID-19 patients: with therapeutic introduction of an oral hyaluronan inhibitor in the prevention of "Induced Hyaluronan Storm" Syndrome

Michael A. Mong^{1*}, Jacob A. Awkal^{2,3*}, Paul E. Marik⁴

¹Department of Surgery, VA North Texas Health Care System Dallas, TX 75216, USA

²Department of Surgery, University of Texas Southwestern Medical Center, Dallas, TX 75390, USA

³Department of Bioengineering, University of Texas at Dallas, Richardson, TX 75080, USA

⁴Division of Pulmonary and Critical Care Medicine, Eastern Virginia Medical School, Norfolk, VA 23510, USA

*These authors contributed equally to this work

Conflict of Interest: In 2020, Michael Mong filed patent application number 63005439-Systems And Methods For Treating Corona Virus.

Funding Source: No external funding was acquired for this manuscript.

Abbreviations: COVID-19, novel coronavirus disease 2019; SARS-CoV-2, severe acute respiratory syndrome coronavirus 2; HA, hyaluronic acid or hyaluronan; IHS, induced hyaluronan storm; CSS, cytokine storm syndrome; SEB, staphylococcal enterotoxin B

Word count: 2,953

"You may take notes for 20 years, from morning to night at the bedside of the sick, upon the diseases of the viscera, and all will be to you only a confusion of symptoms...a train of incoherent phenomena. Open a few bodies and this obscurity will disappear." -

Marie-François-Xavier Bichat (1771–1802), "The Father of Histology"^[1].

Abstract

Background To date, more than 161,000 people have died from the coronavirus disease 2019 (COVID-19) yet the fundamental drivers of the morbidity and mortality remain uncertain. Clinicians worldwide appear to be at a loss to know how to prevent and treat the severe respiratory distress in these patients effectively. Consequently, the fundamental mechanisms leading to death in high-risk patients with COVID-19 need to be discovered and addressed with urgency. Despite a marked drop in frequency, the post-mortem autopsy remains an essential part of both discovering the cause of death in a particular individual, but also in advancing the science and treatment of disease, especially in the case of novel pathogens such as SARS-CoV-2^[2]. The goal of an autopsy is to discover the cause of death (COD) using a macro/microscopic investigation. Traditionally, the intact organs are carefully removed, inspected, and weighed. Because lung weight is often affected by the cause of death and the last breath occurs very near if not at the moments of death, the evaluation of the lungs is one of the starting points of any COD investigation^[3].

Method A comprehensive search was performed to systematically review all reported autopsy findings in COVID-19 patients in order to better understand the underlying disease mechanisms resulting in death. We then compared these findings with the results of a targeted literature review of hyaluronan in relationship to acute respiratory distress syndrome (ARDS).

Results In total, data from 181 autopsies were identified. From this group, 6 autopsies of COVID-19 patients were selected for a detailed review and statistical analysis. The average lung weight of those who were determined to have died as a result of SARS-CoV-2 was 2196g-approximately 2.5x normal lung weight. Hyaline membranes were consistently identified on histologist sections. A review of the literature reveals that hyaluronan has been associated with the pathophysiology of ARDS since 1967. However, its key role in driving the morbidity and

mortality of the condition has heretofore not been fully recognized.

Conclusions We propose that the induced hyaluronan storm syndrome or IHS, is the model that best addresses the heretofore perplexing respiratory failure that is the proximal cause of death in a minority, but ever rising number, of patients. In addition to treating and preventing IHS in currently infected individuals now; an aggressive research effort should be undertaken to discover why the majority of individuals who are exposed to the virus are either minimally or asymptomatic, while a minority of high-risk individuals rapidly progress to respiratory failure and death.

Keywords Systematic review; COVID-19; SARS-CoV-2; Hyaline Membrane; Hyaluronan; Acute Respiratory Distress Syndrome; ARDS; Autopsy; IHS; Induced Hyaluronan Storm Syndrome; COD; Cause of Death

Introduction

To date no coherent model has emerged to explain, prevent, or treat the rapid respiratory failure that is the proximal cause of death in a minority of 2019 novel coronavirus (2019-nCoV; SARS-CoV-2; COVID-19) patients. Similarly, this fact remains true for acute respiratory distress syndrome (ARDS) first described by Ashbaugh in 1967^[4], the severe acute respiratory syndrome (SARS) outbreak in 2002, and the Middle East respiratory syndrome (MERS) in 2012.

Clearly, a small subset of infected individuals rapidly progress, often in a few hours to a few days, from initial symptoms of fever and dyspnea, to full-blown respiratory failure requiring mechanical ventilation, while others remain essentially asymptomatic. Once placed on a ventilator, the death rate has been reported to be between 37 to 62 percent and up to 80 percent depending on age and other risk factors^[5]. Currently, the explanation offered to explain these events has been the cytokine storm syndrome (CSS)^[6]. However, this model is lacking in many

respects, and does not readily lead to a broad based hypothesis that can be tested immediately under the current FDA investigational drug expanded access/compassionate use pathway.

Using a systems biology framework^[7], we conducted a comprehensive review of autopsy reports relating to SARS-CoV-2 deaths, and reviewed the literature concerning hyaluronan with respect to acute respiratory distress syndrome (ARDS). We found that there is a consistent and statistically significant increase in the reported lung weights at autopsy in confirmed SARS-CoV-2 victims with histologic findings of “hyaline membranes” that have classically been described in ARDS, SARS, and MERS autopsies as well. Most significantly, in the first report of two complete autopsies in SARS-CoV-2 in the English language literature, the observed lung weight of a victim with a positive nasopharyngeal and bilateral lung parenchymal swab, by rRT-PCR for SARS-CoV-2, weighed 2,452g - approximately 2.5 times the normal adult lung weight. These lungs were described at autopsy to be as a “bag of water” (personal communication)^[8].

In sharp contrast and most importantly, a 42-year-old obese man was determined to have died with SARS-CoV-2 but not because of SARS-CoV-2. At postmortem examination, the nasopharyngeal swab tested positive for SARS-CoV-2 but there was a negative lung parenchymal swab, with normal lung weights and findings of acute bronchopneumonia, and no hyaline membranes. We believe this may serve to confirm the unique cause of death induced by the super-normal outpouring of hyaluronan over a short time interval and in the confined space of the human chest cavity. We propose to define a new model of the induced hyaluronan storm (IHS) syndrome, as the most comprehensive, specific, and actionable paradigm to frame and address the global SARS-CoV-2 crisis and specifically, to prevent death in high-risk groups.

Modig and Hällgren in 1989, elegantly demonstrated that hyaluronic acid can be induced within minutes in alveolar fluids and leads to a dose dependent reduction in pulmonary

oxygenation index, PaO₂/FaO₂. They further demonstrated up to an 8080% increase in alveolar hyaluronic acid concentration in ARDS patients compared to controls. Stating that “hyaluronic acid is the most powerful water(edema)-binding substance in the body”, they put forth a “humoral” and “biochemical-physiological” hypothesis of ARDS^[9]. Others have recently detailed the central role of hyaluronic acid in human respiratory disease, in which viral infections lead to marked and rapid increase /in hyaluronic acid concentrations^{[10], [11], [12]}.

McKallip, et al. reported in 2013, in an *in vitro* and animal model of ARDS that “targeting hyaluronic acid synthesis might be a novel target for the treatment or reduction of...induced lung injury”. Using an elegant combination of cell based and murine studies, they showed it was possible to profoundly suppress the production of hyaluronan by inhibiting the three isoenzymes of hyaluronan synthase- HAS-1, HAS-2, and HAS-3 with 4-MU (4-methylumbelliferone)^[13].

A follow up study by the same group went on to show that “4-MU (a non-toxic molecule) reduces expression of HAS-1, HAS-2, and HAS-3 (the enzymes that produce HA), and reduced levels of HA in the lungs of SEB-exposed mice” and that “4-MU (4-methylumbelliferone) treatment led to a reduction in SEB-induced lung permeability, and reduced cytokine production”^[14].

Bray and others in 1991 demonstrated in a bleomycin-induced lung injury model, maximal hyaluronan content was reached after seven days and was 14.6 fold the normal value^[15]. Reeves et al. in 2020, showed that human lung fibroblasts (HLFs) treated with viral mimetic polyinosine-polycytidylic acid, a Toll-like receptor 3 agonist, encourages the accumulation of hyaluronan-rich extracellular matrix (ECM) and enhances monocyte and lymphocyte binding. It was shown that the activity of mast cells (innate immune cells), particularly in acute respiratory infections such as respiratory syncytial virus (RSV), can lead to the formation of a hyaluronan-enriched ECM. Further emphasizing that RSV infections of HLFs

encourages inflammation via HA-dependent mechanisms that enhance mast cell protease expression through direct contact with the ECM^[16]. It has been shown that hyaluronan and its various degradation products *in vitro* are a significant contributor to the immunomodulatory functions of the ECM in both acute and chronic respiratory diseases.

Paul Bollyky, M.D., PhD. and Nadine Nagy PhD. et al., researchers at Stanford, extensively reviewed the use of Cantabilin® in 2015 in both animal and human studies in terms of its mechanism of action, pharmacokinetics, and safety with respect to cancer and autoimmunity. These researchers reported on eight human studies dating back to 1978 involving HA and cancer. They concluded that "there is a potential for hymecromone to be developed and repurposed as a safe, long-term adjunctive therapy for cancer treatment or other potential indication."^[17]

Methods

Study Type A systematic comprehensive review of COVID-19 autopsy reports and scientific literature using key search terms.

Inclusion Criteria The inclusion criteria of this study were: COVID-19 autopsy reports; search results involving the selected terms COVID-19, Autopsy, Hyaluronan, Hyaluronic Acid, ARDS.

Exclusion Criteria Studies were excluded if they lacked (i) corresponding outcome parameters or research data or (ii) did not have available full text.

Search Strategy We conducted a targeted systematic review following the PRISMA flow diagram methodology. J.A.A. and M.A.M. systematically searched the electronic databases, PubMed and Scopus, for eligible reports following the PRISMA methodology (flow diagrams and search terms are listed in Figure 1). We included full reports with original data and applied no exclusions based on language. The search deadline was on April 12, 2020.

Data Extraction The elements extracted included sample size, location, measurement indicators of lung, spleen, liver, and the circulatory system. Literature was reviewed independently by two researchers (J.A.A. and M.A.M.). Autopsy reports were also screened for pre-existing conditions (n = 2 subjects with lung cancer were excluded). The primary outcome of interest was SARS-CoV-2 autopsy results with reference to lung weights and presence of hyaline membranes. Mechanisms related to hyaluronan's role in ARDS pathology were selected for detailed analysis.

Data Collection and Quality Assessment Relevant data elements were identified from each publication and recorded in Microsoft Excel (Microsoft Corporation, Redmond, WA, USA) and Zotero (George Mason University, Fairfax, VA, USA). All citations extracted from the PubMed or Scopus electronic databases were deemed to be of sufficient scientific quality.

Data Synthesis and Analysis We summarized the autopsy findings and compared the association between each outcome from the relevant studies. Further collating these results with citations related to hyaluronan and ARDS. These findings were compiled in an outcome status report in the form of a table listing the significant findings. Statistical analysis was carried out with respect to both COVID-19, ARDS, and normal lung weights.

Results

Search Results We identified 22 eligible publications after removing duplicates (Figure 1). Of these, 18 publications were excluded after screening titles and abstracts. Of the remaining, 5 publications were reviewed with full-text reads, one publication that did not meet the inclusion criteria was excluded, leaving 4 publications for the analyses. All publications were considered of sufficient scientific quality. All anatomic and histologic findings in SARS-CoV-2 reports were collated and compiled into Table 1. Case 1 (Barton) with bilateral lung parenchymal swabs positive by rRT-PCR for SARS-CoV-2 had a lung weight of 2,452g - approximately 2.5 times the normal adult lung weight and showed the presence of hyaline membranes and bilateral diffuse alveolar damage. Case 2, (Barton) autopsy revealed positive nasopharyngeal but negative bilateral lung parenchymal swabs by rRT-PCR for SARS-CoV-2 and showed no hyaline membranes, lung weight was documented at a normal 1191g.

Findings	Title	
	COVID-19 Autopsy 1, Xu	
Lung	<ul style="list-style-type: none"> Bilateral diffuse alveolar damage Cellular fibromyxoid exudates Right Lung: desquamation of pneumonocytes hyaline membrane formation Left Lung: pulmonary oedema, hyaline membrane formation Interstitial mononuclear inflammatory infiltrates dominated by lymphocytes Multinucleated syncytial cells with atypical enlarged pneumonocytes (large nuclei, amphophilic granular cytoplasm and prominent nucleoli in intra alveolar spaces No intranuclear or intracytoplasmic viral inclusions X-ray images of rapid progression of pneumonia and lymphopenia 	
Liver	<ul style="list-style-type: none"> Moderate microvascular steatosis and mild lobular and portal activity 	
Vascular	<ul style="list-style-type: none"> Peripheral CD4 and CD8 T cells were substantially reduced, status was hyperactivated high proportions of HLA-DR (CD4 3-47%) and CD38 (CD8 39-4%) double-positive fractions increased concentration of highly proinflammatory CCR6+ Th17 in CD4 T cells CD8 T cells harbored high concentrations of cytotoxic granules 31.6% cells were perforin positive; 64.2% cells were granulysin positive; 30.5% cells were granulysin and perforin positive++ Overactivation of T cells, manifested by an increase of Th17 and high cytotoxicity of CD8 T cells 	
	COVID-19 Autopsy 2, Xiahong	
Lung	<ul style="list-style-type: none"> Alveolar exudative inflammation, thickness of alveolar wall, flesh degeneration Interstitial inflammation and fibrosis Focal bleeding, monocytes and macrophages were the main exudate cells in the alveolar cavity, inflammatory cells infiltration Transparent membrane formation (hyaline membrane) Alveolar capillaries dilated and congested with transparent thrombosis and microvessels & interstitial fibrosis Hyperplastic type II alveolar epithelial cells enlargement, degenerated, and necrotic expressing epithelial cell markers keratin (CK) and thyroid transcription factor 1 (TTF1) More CD68-positive macrophage infiltration in alveolar septum and alveolar cavity. Small number of CD4-positive T cells were in the alveolar septum and interstitial lung No CD8-positive T cells and CD20-positive B cells were seen 	
Spleen & Kidney	<ul style="list-style-type: none"> Number of splenic lymphocytes were significantly reduced Degeneration and necrosis visible with reduced bone marrow three-lineage cells Hepatic cell degeneration and focal necrosis with swollen glomerular endothelial cells Small amount of protein exudate seen in balloon cavity with transparent thrombus seen in capillaries Renal tubular epithelial cells edema, vacuolar degeneration, and shedding, and protein and pigment ducts visible in lumen 	
Vascular	<ul style="list-style-type: none"> Cardiomyocyte hypertrophy, degeneration, and necrosis Mild interstitial hyperemia, edema, infiltration of a small number of lymphocytes, monocytes and neutrophils Some myocardial fibers exhibited swelling and dissolution Macrophage and a small number of CD4-positive T cells infiltrated into myocardium PCR detection did not detect COVID-19 virus component in myocardial tissue 	
	COVID-19 Autopsy 3, Barton	
Lung	<p>Case 1, 77-Year-Old Man</p> <ul style="list-style-type: none"> Combined lung weight: 2452g Firm and edematous right pleural adhesions No effusions, and diffuse alveolar damage The most common histopathologic correlate of ARDS is diffuse alveolar damage, characterized by hyaline membrane formation in the alveoli in the acute stage Lung parenchymal swabs: + for COVID-19 Lung parenchymal swabs: + for COVID-19 	<p>Case 2, 42-Year-Old Man</p> <ul style="list-style-type: none"> Combined lung weight: 1191g No adhesions or effusions Lung parenchymal swabs: + for COVID-19 Lung parenchymal swabs: - for COVID-19
Liver	<ul style="list-style-type: none"> Hepatic centrilobular steatosis Remote cholecystectomy Liver weight: 2232g Right upper quadrant adhesions, no pancreas abnormalities 	<ul style="list-style-type: none"> Advanced hepatic cirrhosis Remote cholecystectomy Liver weight: 1683g
Vascular	<ul style="list-style-type: none"> No adhesions, effusions, or thrombi 	

Table 1. Summary of COVID-19 autopsies extracted from the publications included in the study.

Findings were reported as presented in the autopsy reports.

Statistical Analysis Average lung weights were plotted on MATLAB (MathWorks, Natick, MA, USA) and Microsoft Excel (Microsoft Corporation, Redmond, WA, USA). Post-hoc analysis using the Tukey HSD (Honestly Significant Difference) to indicate group statistical significance, provided 95 percent confidence intervals between the groups. It is important to note that performing the Tukey HSD test requires a studentized range distribution. Due to limited number of lung weights in confirmed IHS± SARS-CoV-2 victims, we cannot determine a p-value at this point. However, it is clearly observed that the lung weights seen between IHS+ and IHS- autopsies is 2:1, which we believe is indicative of a significant difference. One COVID-19 IHS+ case was recorded with a combined lung 1940g^[18].

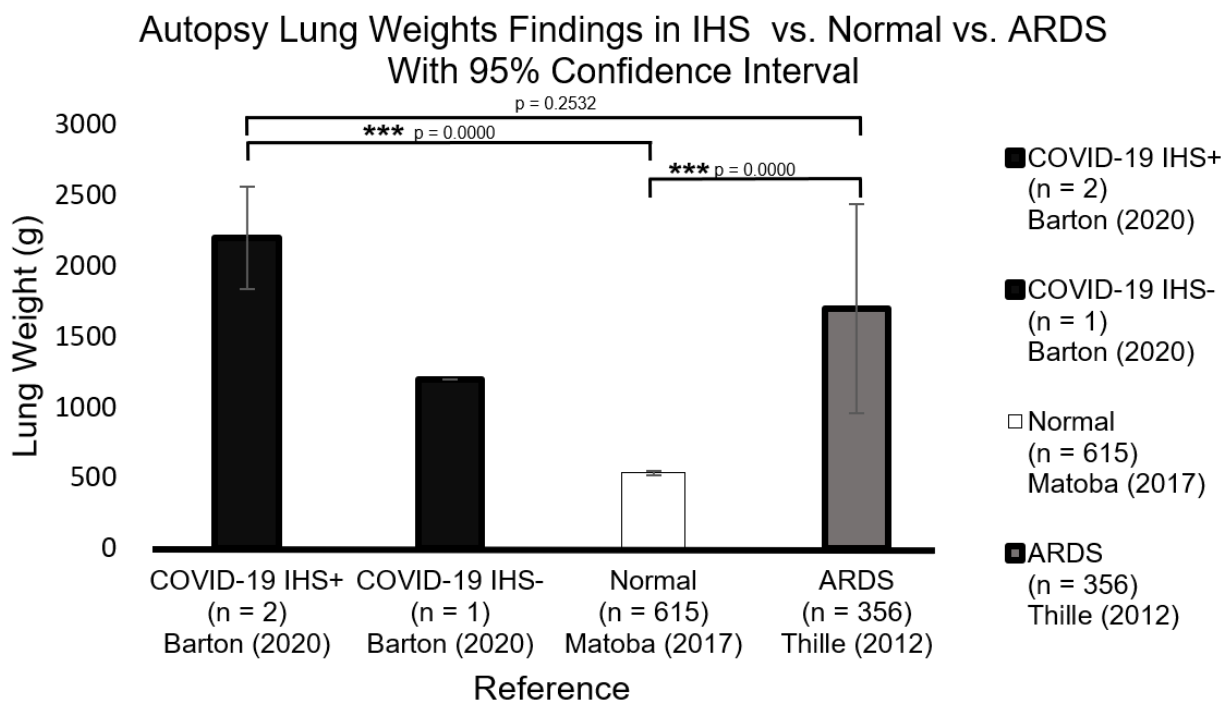


Figure 2. Statistical analysis of lung weights in IHS±, normal, and ARDS autopsies. A one-way ANOVA was performed followed by a post-hoc Tukey HSD. Because SARS-CoV-2 autopsy lung weights were limited, a small sample size was analyzed for IHS+ victims.

Discussion

We employed a systems biology^[7], rather than a reductionist approach, to better characterize and understand the mechanisms associated with the morbidity and mortality associated with COVID-19. We propose that a hyperacute rise in hyaluronan concentration is the key driver of morbidity and mortality in SARS-CoV-2 patients. The induced, sudden, and overwhelming increase in concentration in HA, directly leads to a fatal accumulation of water in the lung parenchyma, overwhelming the body's defense mechanisms, causing rapid asphyxia and death, not unlike drowning. No interventions directed toward the down stream effects of this massive accumulation of hyaluronan and requisite water can prevent the consequences of this singular hydrostatic event.

Under appreciated and neglected since the first description of the clinical features of ARDS based on careful autopsy results in 1967^[4], the morphologic and spacial implications of the sudden outpouring of hyaluronic acid and it's sequestration of water in the alveolar environment, has not been fully appreciated and specifically addressed. There are many ways that an insult, and the response to that insult, can be characterized and quantified-morphologically, physiologically, molecularly, biochemically, and genetically, for example. Unfortunately, the focus currently and historically, has centered on the down stream consequences, and not the critical and key physical dimension and spacial aspects of a large volume of accumulated and misplaced water in the lung. Essentially the lung parenchyma, as a direct consequence of massive increases in hyaluronan, rapidly becomes saturated with water. These shifts in water have been demonstrated to begin to occur within minutes, as a direct result of a variety injuries, and in this case, yet unknown and particularly lethal aspects of the SARS-CoV-2 infection, and can within minutes, lead to changes that result in acute respiratory distress requiring ventilation within hours.

Critically, with respect to the above mechanism, it follows that conventional treatment with positive pressure ventilation and all manner of anti-inflammatory medications can not overcome the physical effects of water saturated lung tissue.

These findings, and numerous others, all suggest that treatments targeting the production of hyaluronan may be life-saving in the present pandemic. The beneficial effects of 4-MU in patients that are currently on ventilators, and certainly in symptomatic patients who have not crossed the line into respiratory failure, is strongly suggested by the extant literature.

Fortunately, evidence exists that 4-MU which has been readily available in European Union as an over the counter product, called Cantabilin®, with a current marketing authorization via the Italian Medicines Agency (AIC no. 02130002) might be available for use.

Given the weight of these findings as well as the long track record of the safe use of 4-methylumbelliferone, and particularly the pressing need and current lack of a specific treatment for COVID-19 ARDS, we propose that those on the front lines, (especially in Italy and Spain) consider immediate use of 4-MU under compassionate use guidelines.

The work of Paul Bollyky, M.D., PhD. and Nadine Nagy PhD. et al., would suggest that 800 mg by mouth three times per day at first sign of infection in confirmed high risk patients might be a reasonable initial dose^[17]. These finding provide a rational for studying the use of 4-methylumbelliferone in COVID-19 induced hyaluronan storm in prospective, double-blinded clinical trials in high-risk patients, which we strongly recommend start in the earliest time frame possible, and encourage all readers to recommend specific protocols for doing so. All drugs have unanticipated and unwanted side effects and great caution must be taken in the clinical application of this or any compound in COVID-19. Certainly, 4-MU should only be used under the direct supervision of skilled physicians.

Conclusion

SARS-CoV-2 infection and COVID-19 disease has resulted in a disastrous pandemic of enormous consequences, the likes of which have not been seen in modern times. We propose that the induced hyaluronan storm syndrome or IHS, is the model that best addresses the heretofore perplexing respiratory failure that is the proximal cause of death in a minority, but ever rising number, of patients. We encourage researchers and clinicians to put our model to the test, and expand upon our early understanding of this disease. In addition to treating and preventing IHS in currently infected individuals now; an aggressive research effort should be undertaken to discover why the majority of individuals who are exposed to the virus are either minimally or asymptomatic, while a minority of high-risk individuals rapidly progress to respiratory failure and death. The answer to this question will have profound implications for our fundamental understanding and approach to disease, and for the individuals and institutions charged with the management of this and future threats to global health and well-being. Foundations have been shaken, and the future will be profoundly shaped by these historic events, as history has been shaped by similar events in the past. Let us hope our collective responses are enlightened, cooperative, and well reasoned^[18]. Future directions include the reporting of further IHS± SARS-CoV-2 lung weights and performing additional autopsies on SARS-CoV-2 victims. We recommend the measurement of hyaluronic acid in serum as a potential indicator of IHS status.

Acknowledgements We thank the Lisa Barton, M.D., Ph.D., for personal communications reviewing specific COVID-19 autopsy findings.

Reference

- [1] Burton JL. A bite into the history of the autopsy. *Forens Sci Med Pathol*. 2005 Dec 1;1(4):277–84.
- [2] Bassat Q, Castillo P, Alonso PL, Ordi J, Menéndez C. Resuscitating the Dying Autopsy. *PLoS Med* [Internet]. 2016 Jan 12 [cited 2020 Apr 10];13(1). Available from: <https://www.ncbi.nlm.nih.gov/pmc/articles/PMC4710495/>
- [3] Estimating normal lung weight measurement using postmortem CT in forensic cases. *Legal Medicine*. 2017 Nov 1;29:77–81.
- [4] Ashbaugh DavidG, Boyd Bigelow D, Petty ThomasL, Levine BernardE. ACUTE RESPIRATORY DISTRESS IN ADULTS. *The Lancet*. 1967 Aug 12;290(7511):319–23.
- [5] Bhatraju PK, Ghassemieh BJ, Nichols M, Kim R, Jerome KR, Nalla AK, et al. Covid-19 in Critically Ill Patients in the Seattle Region – Case Series. *New England Journal of Medicine*. 2020 Mar 30;0(0)
- [6] Konig MF, Powell M, Staedtke V, Bai R-Y, Thomas DL, Fischer N, et al. Targeting the catecholamine-cytokine axis to prevent SARS-CoV-2 cytokine storm syndrome. *medRxiv*. 2020 Apr 8;2020.04.02.20051565.
- [7] Tavassoly I, Goldfarb J, Iyengar R. Systems biology primer: the basic methods and approaches. Kolch W, Fey D, Ryan CJ, editors. *Essays in Biochemistry*. 2018 Oct 26;62(4):487–500.
- [8] Barton LM, Duval EJ, Stroberg E, Ghosh S, Mukhopadhyay S. COVID-19 Autopsies, Oklahoma, USA. *Am J Clin Pathol* [Internet]. [cited 2020 Apr 16]; Available from: <https://academic.oup.com/ajcp/article/doi/10.1093/ajcp/aqaa062/5818922>
- [9] Modig J, Hällgren R. Increased hyaluronic acid production in lung—a possible important factor in interstitial and alveolar edema during general anesthesia and in adult respiratory distress syndrome. *Resuscitation*. 1989 Jun;17(3):223–31.
- [10] Lauer ME, Dweik RA, Garantziotis S, Aronica MA. The Rise and Fall of Hyaluronan in Respiratory Diseases [Internet]. Vol. 2015, *International Journal of Cell Biology*. Hindawi; 2015

[cited 2020 Apr 4]. Available from: <https://www.hindawi.com/journals/ijcb/2015/712507/>

[11] Johnson P, Arif AA, Lee-Sayer SSM, Dong Y. Hyaluronan and Its Interactions With Immune Cells in the Healthy and Inflamed Lung. *Front Immunol* [Internet]. 2018 [cited 2020 Apr 17];9. Available from: <https://www.frontiersin.org/articles/10.3389/fimmu.2018.02787/full>

[12] Bell TJ, Brand OJ, Morgan DJ, Salek-Ardakani S, Jagger C, Fujimori T, et al. Defective lung function following influenza virus is due to prolonged, reversible hyaluronan synthesis. *Matrix Biol*. 2019 Jul;80:14–28.

[13] McKallip RJ, Fisher M, Do Y, Szakal AK, Gunthert U, Nagarkatti PS, et al. Targeted Deletion of CD44v7 Exon Leads to Decreased Endothelial Cell Injury but Not Tumor Cell Killing Mediated by Interleukin-2-activated Cytolytic Lymphocytes. *J Biol Chem*. 2003 Oct 31;278(44):43818–30.

[14] McKallip RJ, Hagele HF, Uchakina ON. Treatment with the Hyaluronic Acid Synthesis Inhibitor 4-Methylumbelliferone Suppresses SEB-Induced Lung Inflammation. *Toxins (Basel)*. 2013;5(10):1814-1826. doi:10.3390/toxins5101814

[15] Bray BA, Sampson PM, Osman M, Giandomenico A, Turino GM. Early Changes in Lung Tissue Hyaluronan (Hyaluronic Acid) and Hyaluronidase in Bleomycin-induced Alveolitis in Hamsters. *American Review of Respiratory Disease* [Internet]. 2012 Dec 17 [cited 2020 Apr 19]; Available from: <https://www.atsjournals.org/doi/abs/10.1164/ajrccm/143.2.284>

[16] Reeves SR, Barrow KA, Rich LM, White MP, Shubin NJ, Chan CK, et al. Respiratory Syncytial Virus Infection of Human Lung Fibroblasts Induces a Hyaluronan-Enriched Extracellular Matrix That Binds Mast Cells and Enhances Expression of Mast Cell Proteases. *Front Immunol* [Internet]. 2020 Jan 28 [cited 2020 Mar 28];10. Available from: <https://www.ncbi.nlm.nih.gov/pmc/articles/PMC6997473/>

[17] Nagy N, Kuipers HF, Frymoyer AR, et al. 4-Methylumbelliferone Treatment and Hyaluronan Inhibition as a Therapeutic Strategy in Inflammation, Autoimmunity, and Cancer. *Frontiers in Immunology*. 2015;6. doi:10.3389/fimmu.2015.00123

[18] Liu Q, Wang RS, Qu GQ, Wang YY, Liu P, Zhu YZ, et al. Gross examination report of a COVID-19 death autopsy. *Fa Yi Xue Za Zhi*. 2020 Feb;36(1):21–3.

[19] Gully PR. Pandemics, regional outbreaks, and sudden-onset disasters. *Healthc Manage Forum*. 2020 Feb 5;0840470420901532.

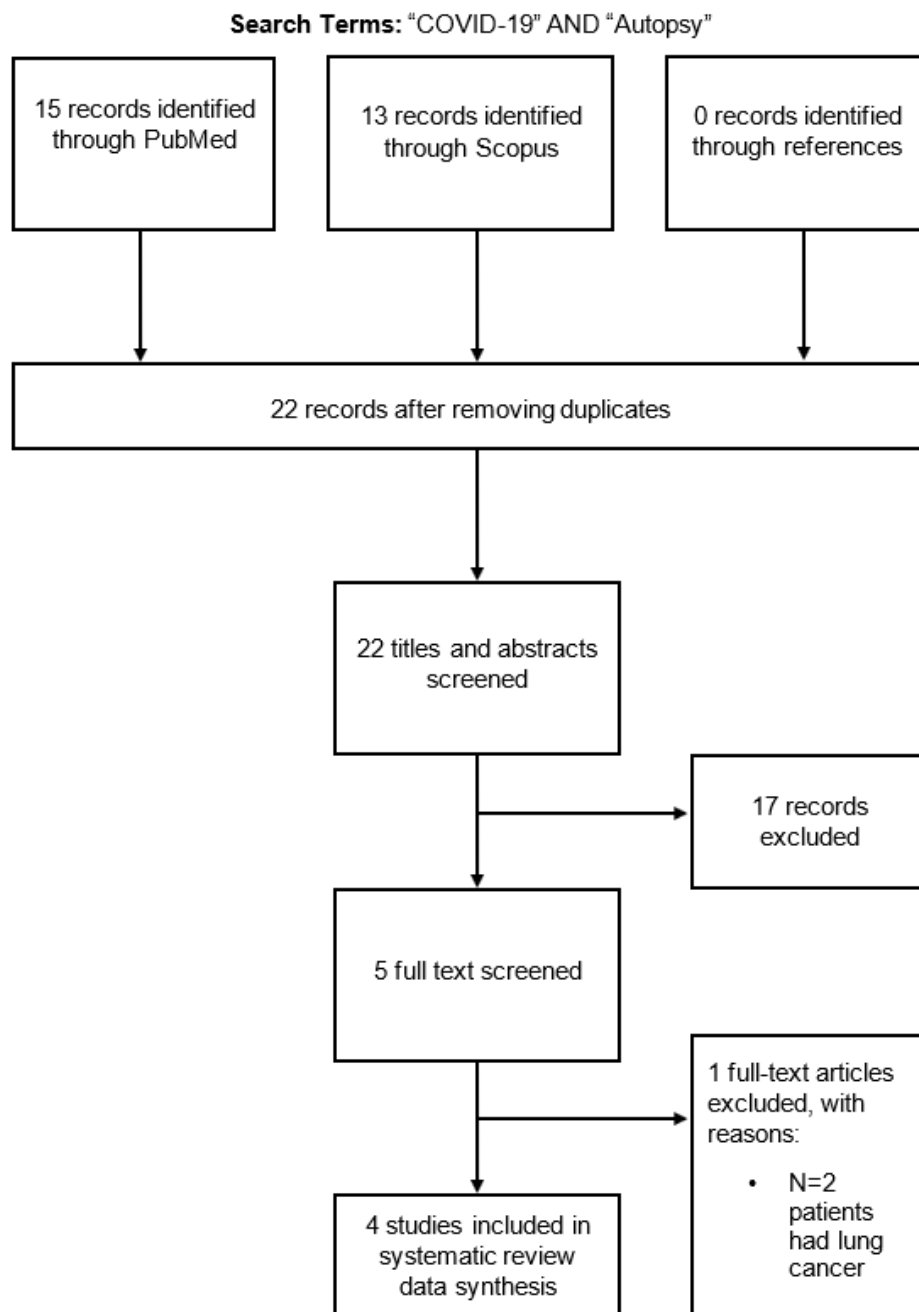


Figure 1. Flow chart of study selection

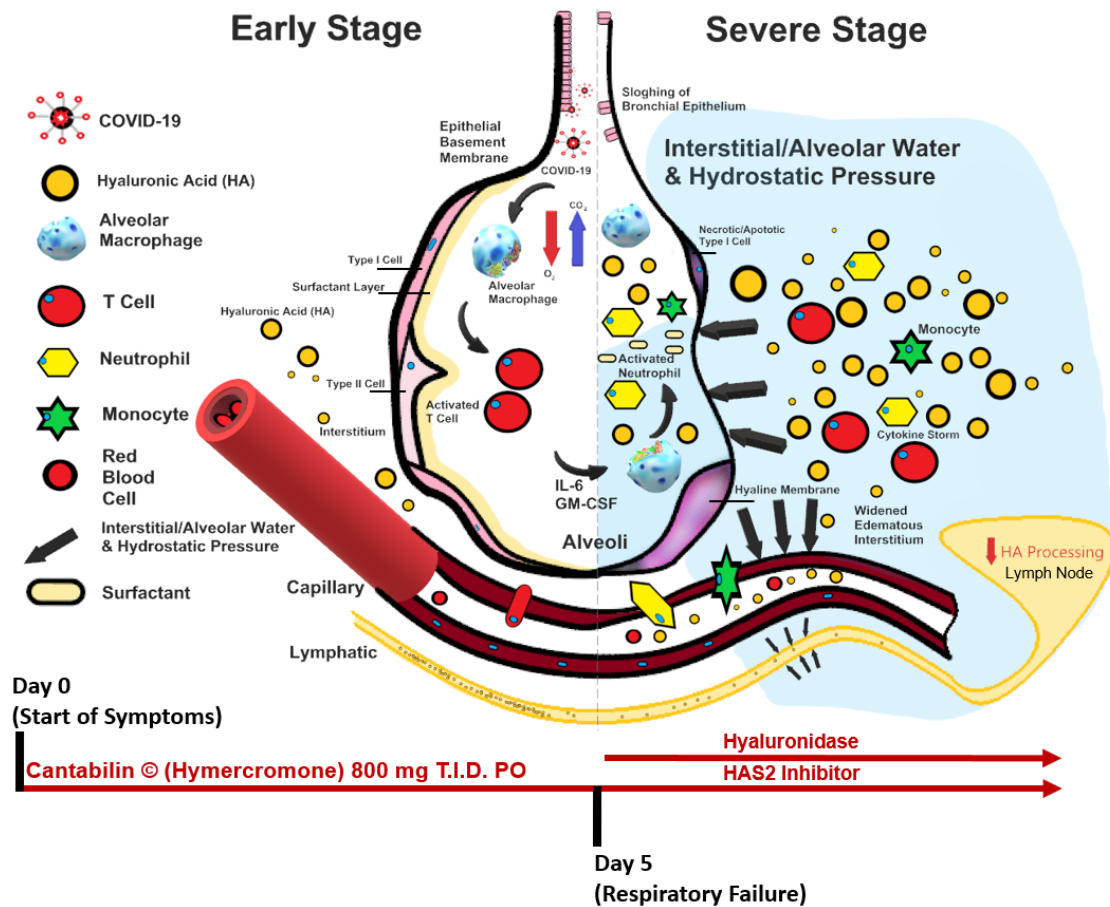


Figure 3. Schematic of the progression of COVID-19 infection and potential interventions. After a certain period, SARS-CoV-2 causes non-severe symptoms, therefore eliciting protective immune response. In this period, strategies to boost the immune response should be applied before the infected individual enters the severe stage, when strong damaging inflammatory responses occur, especially in the lung. Before this stage, the inhibition of hyaluronan synthase and elimination of hyaluronan should be considered.

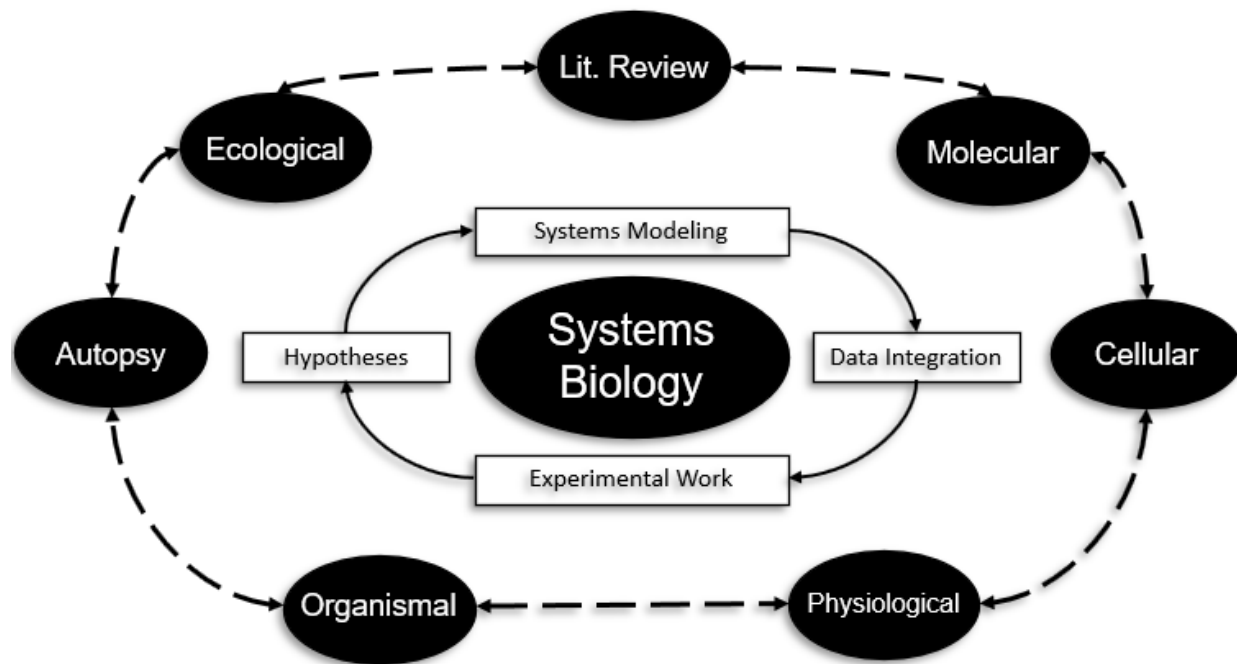
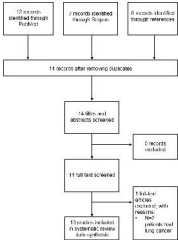


Figure 4. Theoretical framework outlining the elements of a system biology, in contrast to reductionist, approach to complex disease states. Note the inclusion of autopsy as an integral component of this dynamic network.

Search Terms: "COVID-19" AND "Autopsy"



CONV-10-Chapter 4, B1

<p>Prerequisite</p>	<ul style="list-style-type: none"> • History of the storage device • Disk controller hardware • Diskless, nonpartitioned, unformatted, hybrid, partitioned, formatted • RAID array redundancy schemes, hot spare storage functions • Storage array controller characteristics, RAID levels, RAID controller types • RAID controller array and controller port and port characteristics (e.g., SCSI, SAS, SATA, Fibre Channel, iSCSI, InfiniBand, and SATA) and port mode • RAID controller characteristics and functions • RAID controller performance characteristics and applications
<p>Goal</p>	<ul style="list-style-type: none"> • Identify the storage hardware and software used in storage systems
<p>Outcome</p>	<ul style="list-style-type: none"> • Identify RAID levels and RAID array redundancy schemes, RAID controller types • High capacity of RAID controllers (e.g., RAID 0, RAID 1, RAID 5, RAID 6, RAID 10) • RAID controller types and controller port and port characteristics (e.g., SCSI, SAS, SATA, Fibre Channel, iSCSI, InfiniBand, and SATA) and port mode • RAID controller array and controller port and port characteristics (e.g., SCSI, SAS, SATA, Fibre Channel, iSCSI, InfiniBand, and SATA) and port mode • RAID controller array and controller port and port characteristics (e.g., SCSI, SAS, SATA, Fibre Channel, iSCSI, InfiniBand, and SATA) and port mode

CONV-10-Chapter 4, B2

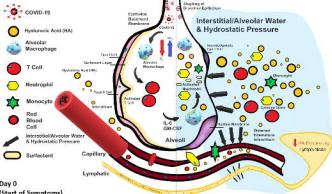
<p>Prerequisite</p>	<ul style="list-style-type: none"> • RAID controller hardware and software used in storage systems • RAID controller array and controller port and port characteristics (e.g., SCSI, SAS, SATA, Fibre Channel, iSCSI, InfiniBand, and SATA) and port mode • RAID controller array and controller port and port characteristics (e.g., SCSI, SAS, SATA, Fibre Channel, iSCSI, InfiniBand, and SATA) and port mode • RAID controller array and controller port and port characteristics (e.g., SCSI, SAS, SATA, Fibre Channel, iSCSI, InfiniBand, and SATA) and port mode • RAID controller array and controller port and port characteristics (e.g., SCSI, SAS, SATA, Fibre Channel, iSCSI, InfiniBand, and SATA) and port mode • RAID controller array and controller port and port characteristics (e.g., SCSI, SAS, SATA, Fibre Channel, iSCSI, InfiniBand, and SATA) and port mode
<p>Goal</p>	<ul style="list-style-type: none"> • Identify the storage hardware and software used in storage systems • RAID controller array and controller port and port characteristics (e.g., SCSI, SAS, SATA, Fibre Channel, iSCSI, InfiniBand, and SATA) and port mode • RAID controller array and controller port and port characteristics (e.g., SCSI, SAS, SATA, Fibre Channel, iSCSI, InfiniBand, and SATA) and port mode • RAID controller array and controller port and port characteristics (e.g., SCSI, SAS, SATA, Fibre Channel, iSCSI, InfiniBand, and SATA) and port mode
<p>Outcome</p>	<ul style="list-style-type: none"> • RAID controller array and controller port and port characteristics (e.g., SCSI, SAS, SATA, Fibre Channel, iSCSI, InfiniBand, and SATA) and port mode • RAID controller array and controller port and port characteristics (e.g., SCSI, SAS, SATA, Fibre Channel, iSCSI, InfiniBand, and SATA) and port mode • RAID controller array and controller port and port characteristics (e.g., SCSI, SAS, SATA, Fibre Channel, iSCSI, InfiniBand, and SATA) and port mode • RAID controller array and controller port and port characteristics (e.g., SCSI, SAS, SATA, Fibre Channel, iSCSI, InfiniBand, and SATA) and port mode

CONV-10-Chapter 5, B1

<p>Prerequisite</p>	<ul style="list-style-type: none"> • RAID controller hardware and software used in storage systems • RAID controller array and controller port and port characteristics (e.g., SCSI, SAS, SATA, Fibre Channel, iSCSI, InfiniBand, and SATA) and port mode • RAID controller array and controller port and port characteristics (e.g., SCSI, SAS, SATA, Fibre Channel, iSCSI, InfiniBand, and SATA) and port mode • RAID controller array and controller port and port characteristics (e.g., SCSI, SAS, SATA, Fibre Channel, iSCSI, InfiniBand, and SATA) and port mode 	<ul style="list-style-type: none"> • RAID controller hardware and software used in storage systems • RAID controller array and controller port and port characteristics (e.g., SCSI, SAS, SATA, Fibre Channel, iSCSI, InfiniBand, and SATA) and port mode • RAID controller array and controller port and port characteristics (e.g., SCSI, SAS, SATA, Fibre Channel, iSCSI, InfiniBand, and SATA) and port mode
<p>Goal</p>	<ul style="list-style-type: none"> • RAID controller hardware and software used in storage systems • RAID controller array and controller port and port characteristics (e.g., SCSI, SAS, SATA, Fibre Channel, iSCSI, InfiniBand, and SATA) and port mode • RAID controller array and controller port and port characteristics (e.g., SCSI, SAS, SATA, Fibre Channel, iSCSI, InfiniBand, and SATA) and port mode 	<ul style="list-style-type: none"> • RAID controller hardware and software used in storage systems • RAID controller array and controller port and port characteristics (e.g., SCSI, SAS, SATA, Fibre Channel, iSCSI, InfiniBand, and SATA) and port mode • RAID controller array and controller port and port characteristics (e.g., SCSI, SAS, SATA, Fibre Channel, iSCSI, InfiniBand, and SATA) and port mode
<p>Outcome</p>	<ul style="list-style-type: none"> • RAID controller hardware and software used in storage systems • RAID controller array and controller port and port characteristics (e.g., SCSI, SAS, SATA, Fibre Channel, iSCSI, InfiniBand, and SATA) and port mode • RAID controller array and controller port and port characteristics (e.g., SCSI, SAS, SATA, Fibre Channel, iSCSI, InfiniBand, and SATA) and port mode 	

Early Stage

Severe Stage



Day 0
(Start of Symptoms)

Cantabilin © (Hymecromone) 800 mg T.I.D. PO

Hyaluronidase

HAS2 inhibitor

Day 5

(Respiratory Failure)

